Solvent –solute and Non-covalent interactions on bis(4-Piperidinonium ethyl ketal) oxalate compound:DFT calculations and in Silico Drug-Target Profiling

Mahdi Jemai, Noureddine Issaoui, Thierry Roisnel, Aleksandr S. Kazachenko, Omar Al-Dossary, Houda Marouani

Solvent –solute and Non-covalent interactions on bis(4-Piperidinonium ethyl ketal) oxalate compound:DFT calculations and *in Silico* Drug-Target Profiling

Mahdi Jemai[a], Noureddine Issaoui[b,*], Thierry Roisnel[c], Aleksandr S. Kazachenko[d,e], Omar Al-Dossary[f], Houda Marouani[a]

[a]*Laboratory of Material Chemistry, Faculty of Sciences of Bizerte, University of Carthage, Bizerte, Tunisia*

[b]*Laboratory of Quantum and Statistical Physics (LR18ES18), Faculty of Sciences, University of Monastir, Monastir 5000, Tunisia;*

[c]*Univ. Rennes, CNRS, ISCR (Institut des Sciences Chimiques de Rennes) – UMR 6226, F-35000 Rennes, France*

[d]*Siberian Federal University, pr. Svobodny 79, Krasnoyarsk, 660041 Russia*

[e]*Institute of Chemistry and Chemical Technology, Krasnoyarsk Scientific Center, Siberian Branch, Russian Academy of Sciences, Akademgorodok, 50, bld.24, Krasnoyarsk, 660036 Russia.*

[f] *Departement of Physics and Astronomy, College of Science, King Saud University, BO Box 2455, Riyadh 11451, Saudi Arabia*

*Corresponding author: issaoui_noureddine@yahoo.fr (N. ISSAOUI)

Highlight

- Synthesis of a novel, purely organic compound $(C_7H_{14}NO_2)_2(C_2O_4)$.
- Crystallographic study of the atomic arrangement illustrates bidimensional network
- A theoretical study was carried out to map the role of non-covalent interactions in maintaining the crystal structure.
- *In Silico* Therapeutic-target profiling shows the role of combining organic molecules for synthesizing new compounds with improved and more interesting biological properties than the initial reagents.

Author Contributions:

Mahdi Jemai : Conceptualization, methodology, software, formal analysis, writing—original draft preparation

Noureddine Issaoui : Conceptualization, methodology, software, writing—review and editing, supervision, validation,

Thierry Roisnel : Conceptualization, software, validation, data curation

Aleksandr S. Kazachenko: Conceptualization, formal analysis, validation,

Omar Al-Dossary:, Conceptualization, validation, supervision,

Houda Marouani: Conceptualization, validation, formal analysis, writing—review and editing, supervision,

ABSTRACT

In the present paper, we deliver the synthesis, experimental results, and theoretical examination of a newly developed organic supramolecular compound, entitled bis(4-Piperidinonium ethyl ketal) oxalate, with the subsequent chemical formula: $(C_7H_{14}NO_2)_2(C_2O_4)$, denoted by 4PEKOX.The stoichiometric 2:1 ratio of 4-Piperidinone ethyl ketal with oxalic acid, and the slow evaporation that follows, produce this new material. X-ray diffraction was carried out to identify the 4PEKOX asymmetric unit and its two-dimensional lattice. The attachment between 4-Piperidinonium ethyl ketal cations and oxalate anions is provided by N(C)-H...O H-bonds forming supramolecular units of type $R_2^2(8)$, $R_1^2(5)$ and $R_2^1(6)$. The inter-molecular interactions that contribute to crystal packing have been assessed through the use of the HS; the percentage participation of each interaction was presented as two-dimensional fingerprints. The infrared (IR) and UV-Visible spectroscopy allowed us to identify the functional groups and study the optical properties of 4PEKOX. Experimental investigations have been combined with quantum chemical calculations to confirm and evaluate the properties of 4PEKOX from a theoretical perspective, allowing us to explain and examine in detail the electronic transfer, polarity, atomic charges and the role of non-covalent interactions in this new compound. Secondly, the expected therapeutic effect of 4PEKOX as an organic supramolecular compound was studied using the molecular docking technique. We examined the effect of 4PEKOX on the SARS-CoV-2 (7JTL) protein and measured their interaction energy with it, comparing it with the energies of oxalic acid and heterocyclic amine separately with the same protein to show the evolution imposed by synthesis through the combination of organic molecules to produce supramolecules more reactive than the starting reagents. In this study, Favipiravir was used as a reference due to its potent therapeutic activity against multiple coronaviruses.

Keywords: DFT; Solute-solvent interaction; chemical calculations; Molecular docking; SARS-CoV-2; Favipiravir

1. Introduction

Supramolecular chemistry is the chemistry of intermolecular bonding that encompasses the synthesis and design of supramolecules, which are the association of various chemical species bonded by different types of non-covalent (NC) interactions [1]. Supramolecular chemistry includes a branch known as crystal engineering which allows us to understand these inter-molecular interactions, their crystallographic geometry and how we can apply them to the study of the structure of these new solids [2], it is a particularly effective tool for defining the precise process by which these interactions take place, which has been the focus of recent papers [3-5].In the perspective of crystal engineering, the synthesis of purely organic crystals has become an intense research objective, since the initial discovery of an organic crystal using X-ray diffraction in the 1920s; solid state chemists have become increasingly interested in this type of crystal [6]. Organic crystallization is characterized by its importance in pharmaceutical science [7], drugs development is highly dependent on how these materials are processed and handled [8]. Other applications related to these types of crystals such as biological systems [9,10], electronic manufacturing [11], optoelectronic technologies [12], electrochemistry field [13], etc.

4-Piperidinone ethyl ketal, also known as 1,4-Dioxa-8-azaspiro[4.5]decane, is a heterocyclic organic compound derived from azaspirodecane, it is important to know that heterocyclic chemistry is considered one of the basic classes of medicinal chemistry, heterocycles are present in over 90% of new drugs [14,15]. Azaspirodecane derivatives are among the heterocyclic

compounds used in the pharmaceutical field to produce anti-inflammatory, antioxidant, anticonvulsant, antibacterial and antifungal compounds [16-19].

Oxalic acid (OA) is a strong dicarboxylic acid with a $pKa_1 = 1.25$ and a $pKa_2 = 4.27$, for which it is mostly found in the environment in the form of its conjugated base, oxalate [20]. Fungi, bacteria, plants and animals all produce oxalic acid [21]. In the human body, the natural methabolization of glycine and ascorbic acid leads to the formation of OA [22]. In addition, humans consume a large amount of oxalate in their diet, especially from plant food sources, we must therefore be wary of high consumption of oxalate-rich foods, which have negative effects on health and can particularly affect vegetarians, they make calcium absorption invalid, excessive consumption of oxalate-rich foods leads to hyperoxaluria, which is known to be a potent factor in the accumulation of calcium oxalate stones [23-25].

In the present study we are interested in the synthesis of the new compound bis(4-Piperidinonium ethyl ketal) oxalate, for the reason of studying the structure of this supramolecule and analyzing its related properties and the interaction between the oxalate anion and the 4-Piperidinonium ethyl ketal cation by experimental and quantum chemical methods, as well as the expected therapeutic effect of 4PEKOX.

The aim of this research paper is to draw researchers' attention to the advantages of combining small organic molecules to produce a new supramolecule with more interesting properties than the starting reactive products, and this is what it shows in this manuscript: the evolution of the therapeutic properties of the new compound 4PEKOX compared to the reactive products used in its production.

2. Experimental

2.1. Chemical preparation

The new bis(4-Piperidinonium ethyl ketal) oxalate,$(C_7H_{14}NO_2)_2(C_2O_4)$, was created through the stoichiometric ratio 1:2 mix between oxalic acid and 4-Piperidinone ethyl ketal. 0.5 mmol (0.046 g) of OA and 1 mmol (0.017 mL) of 4-Piperidinone ethyl ketalare put together in a beaker supplemented with 6 mL of water taken as a solvent. The interaction between the solvent and the solutes gives rise to a mixture, the latterhad been magnetically agitated during one hour, and then at 298.15 K, the solution was gradually evaporated. Several days later, colorless prismatic crystals suitable for structuralstudies are formed (Yield 65%). The elemental analyses calculated and found are shown below respectively: C: 51.01%, 51.12%; O: 34.01%, 34.08%; N: 7.44 %, 7.38%. This chemical process can be represented as in **Scheme 1**.

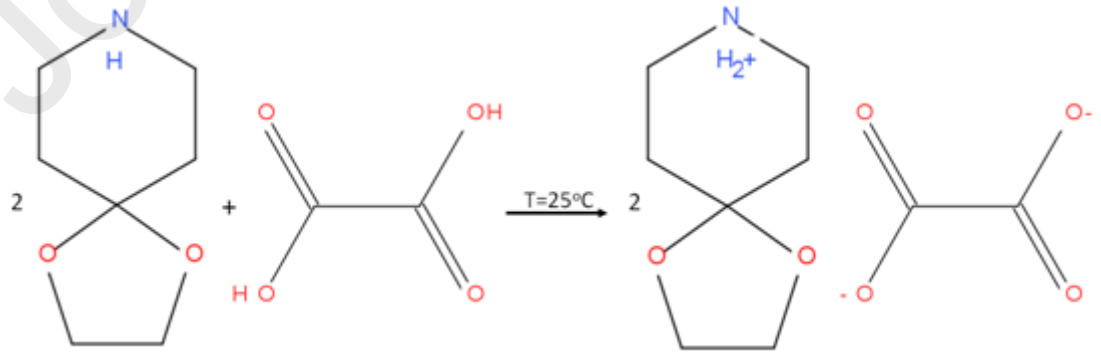

Scheme 1. Chemical reaction of the 4PEKOX formation.

2.2. X-Ray data collection

Single-crystal X-ray diffraction data of the bis(4-Piperidinonium ethyl ketal) oxalate were collected using a diffractometer D8 VENTURE Bruker AXS includes a CCD detector and a Mo Kα X-ray source with a monochromatic wavelength of 0.71073 Å. Through the SADABS program, the multi-scan approach was used to rectify the data [26]. Using WINGX program, SHELXT-2018 allowed us to solve the structure directly, thus providing the positions of all atoms other than hydrogen atoms, and then refined with full-matrix least-square methods based on F^2 (SHELXL-2018) [27]. A different map was used to locate and then refine the nitrogen hydrogen atoms.The other hydrogen atoms were defined as riding, with $U_{iso}(H) = 1.2U_{eq}(C)$ and C—H $_{\underline{methylene}}$ = 0.99. **Table 1** shows the crystallographic data and structure refinements.

2.3. Physical Measurements

Using a Perkin-Elmer Spectrum Two FT-IR Spectrometer, the infrared spectrum was collected between 4000 and 400 cm^{-1} at 298.15 K.

The solid state UV spectroscopy was carried out at 298.15 K between 200 and 500 nm using a Perkin-Elmer Lambda 365 UV-Vis Spectrometer.

2.4. Quantum chemical calculations

The structure of the title compound has been modeled using the GaussView program [28], and then the Gaussian 09 software package was used [29]. The B3LYP/LANL2DZ method was employed to perform all quantum chemical analyses of the electronic structure and optimized geometry of 4PEKOX [30]. The choice of the employed functional, which is Becke's 3-parameter hybrid exchange functional coupled with the Lee-Yang-Parr correlation functional and enriched by empirical dispersion, holds significance in comprehending the intricate electronic properties of the compound under investigation. This functional provides a balanced approach that amalgamates the strengths of different theoretical methodologies to capture essential electronic behaviors, ensuring an accurate representation of the compound's behavior. The optimized structure represents the most stable structure since it does not contain imaginary frequencies in the vibration frequency calculations. En effect, the optimized molecular structure has energy worth -857.307345 a.u and a dipolar moment equal to 13.033 Debye. These calculations allow us to examine the chemical reactivity, polarity, electronic transfer, atomic charges and how NC interactions are involved in this new compound using MEP surface, Mulliken population, frontier orbitals (HOMO-LUMO) and topological AIM, RDG, ELF, LOL and IRI analysis [31-34]. Theoretical chemists have used these programs to map crystal structures and determine the physical characteristics of the new solids. This explains the increasing number of new research publications based on this theoretical method [35-41].

3. Results and Discussion

3.1. Structural comment and supramolecular features

In a monoclinic crystal system with space group $P2_1/c$ the bis(4-Piperidinonium ethyl ketal) oxalate crystallizes with the following cell parameter values: a = 12.1401 (8) Å, b = 6.9253 (5) Å, c = 11.2564 (7) Å, β = 106.433 (2)°, V = 907.71 (11) $Å^3$ and Z = 2. Table 2 displays the

various bond angles and interatomic lengths of anions and cations. As shown in **Figure 1**, the asymmetric unit is formed by a monoprotonated organic cation which is 4-Piperidinonium ethyl ketal and a half- oxalate anion, linked together by two types of hydrogen bonds C-H...O and N-H...O. To describe the atomic arrangement of 4PEKOX we have projected it in the ($\vec{a}$, $\vec{c}$) plane (**Figure 2a**), at first glance, we notice that the organic cations and anions form supramolecules located around an inversion center of coordinates (1/2,1/2,1/2). The oxalate anions grow in layers parallel to the ($\vec{b}$,$\vec{c}$) planesat x = ½, between which are graft the organic cations, forming together a bidimensional network. The conformation displayed in the solid state shows that the heterocyclic structure of the piperidine ring (C1C2C3N4C5C6) is present as a chair conformation with parameters shown values of Q = 0.5612 Å, θ = 2.61° and ϕ = 3.97°.

The structure's cooperation is guaranteed by a network of hydrogen bonds. The different H-bonds present in the structure of 4PEKOX are listed in **Table 3**. H-bonds are subdivided into two types: three hydrogen bonds of type N-H...O with donor-acceptor lengths ranging from 2.7045 (12) to 2.8928 (12)Å, linking the protons of the 4-Piperidinonium ethyl ketal to the oxygen atoms of the oxalate anions, two C-H...O hydrogen bonds with donor-acceptor distances of 3.3873 (13) and 3.4104 (13) Å, relatively long compared to those of the N-H...O type, and therefore weaker than the latter and less involved in maintaining the crystal structure. This pair of types of H-bonds allow to link the organic cations to the oxalate anions forming new supramolecular units of type $R_2^2(8)$,$R_2^1(5)$and $R_2^1(6)$ [42] (**Figure 2b**).

3.2. Hirshfeld Surface Analysis

With the aim to investigate the intermolecular interactions present in the crystal structure of the title substance, we estimated the Hirshfeld surface analysis (d_{norm} mode) and their associated 2D-fingerprint plots using the Crystal Explorer tool [43, 44]. The d_{norm} mode is a 3D-illustrationof the different types of NC interactions found in molecular crystals which are assigned according to a range of colors as follows: the blue color indicates contacts with a longer length than the vdW radius; the white color shows contacts equal to the vdW radius; the red color corresponds to hydrogen bonds (contact is shorter than the vdW radius). The 2D-fingerprint plots allow us to quantify the percentage participation of each intermolecular interaction present in the crystal structure.

Concerning the structure of the bis(4-Piperidinonium ethyl ketal) oxalate, **Figure 3** shows and compares the contribution of interatomic contacts of the title compound and individual cations and anions. The analysis of the Hirshfeld surface of 4PEKOX (All salt) shows that repulsive H...H contacts and H-bonds (O...H/H...O) contacts have the largest contribution with a value of 48.5% and 45.8% respectively of the total HS that appeared in the form of blue and red regions in d_{norm} mode. The important role of N-H…O and C-H…O hydrogen bonds in crystal formation is demonstrated by the high ratio of O...H/H...O contacts.

The contributions of H...O/O...H contacts on the HS of the anion$(C_2O_4)^{2-}$(89.9%) are much higher than that of the organic cation (35.6%), this can be explained by that the oxalate anion contains four oxygen atoms that are all bonded by H-bonds to organic cations, which is due to the strong reactivity of these anions.

3.3. Vibrational Infrared Spectral Analysis

The use of spectroscopic techniques to analyze organic substances allows understanding the vibrational properties of its functional groups. The vibrational modes of the title compound were determined in the crystalline state using experimental absorption spectra, illustrated in **Figure 4**, ranging from 4000 to 400 cm^{-1}. Based on previous studies [45-48], the different absorption bands of 4PEKOX have been deduced.

3.3.1. Vibration Modes of the 4-Piperidinonium ethyl ketal Cation

With regard to the cationic group, this compound's IR absorption spectrum is characterized by an interesting band at 2971 cm^{-1}accorded to the valence vibration of the NH_2^+ group of the piperidine ring, while the deformation vibration of the same group is represented by an intense band at 1582 cm^{-1}. The CH_2 group symmetrical and asymmetrical valence vibrations can be seen by the band around 2897 cm^{-1}, a deformation band at around 750 cm^{-1} is also attributed to the vibration of the CH_2 group. The valence vibration of the CN group of the 4-Piperidinonium ethyl ketal cation is displayed by the band seen at 1315 cm^{-1}. The C-C vibration was considered the source of the band at 1193 cm^{-1}. The intense band at 2971 cm^{-1} indicates the valence vibration of the C-O group of the 1,3-dioxolane ring.

3.3.1. IR vibrations of the oxalate anion $(C_2O_4)^{2-}$

In relation to the anionic group, the IR spectrum has been characterized by a broad band appears at 2415 cm^{-1}related to the valence vibration of the O-H group, with another band appearing at 1397 cm^{-1} due to its deformation vibration. Two further bands of the oxalate anion, located at 1647 and 1267 cm^{-1}, are attributed to the vibration of the C=O and C-O groups, respectively.

3.4. UV-Visible Spectroscopy

4PEKOX's UV-Vis spectrum was collected in the solid-state at room temperature and is shown in **Figure 5a**.We observe that the n−π* charge transition from oxalate anion to4-Piperidinonium ethyl ketal, which results from the interaction between these two organic entities, produces an intense absorption band that appears at 370 nm.We also apply Tauc's method to UV-visible spectroscopy to establish the energy gap of 4PEKOX [49], which introduced an extrapolation process to calculate the energy gap from the variations of $(\alpha h\nu)^2$as a function of hν. This material is classed as a semiconductor, as shown in **Figure 5b**, its Eg value is 2.15 eV.

3.5. HOMO-LUMO Analysis

HOMO stands for the Highest Occupied Molecular Orbital, while LUMO is the Lowest Unoccupied Molecular Orbital. The analysis of the contributions of the atomic groups in these orbitals allows to understand the electron transfer in the compounds to be studied because HOMO-LUMO works as an electron donor-acceptor system, the nucleophilic and electrophilic properties are directly related to HOMO-LUMO orbitals, respectively [50]. These two orbitals are energetically separated by an energy gap ($E_g = E_{HOMO} - E_{LUMO}$), whose value is an important indicator of electrical conductivity [51]. In **Table 4**, we have grouped the global reactivity energy parameters such as E_{HOMO},E_{LUMO}, E_{Gap}, electronic affinity, electrophilicity, ionization potential, electronegativity, chemical potential, Hardness and Softness.

Figure 6 shows the HOMO and LUMO orbitals of 4PEKOX, the red and green colors indicate the positive and negative signs, respectively, of the molecular orbital wave function. The energy difference between the HOMO (−4.6594 eV) and LUMO (−6.8407 eV) orbitals gives the Gap energy, which is 2.1813 eV, in agreement with the value determined by UV-Visible

Spectroscopy using the Tauc method, thus theoretically confirming that 4PEKOX is a semiconductor.

3.6. Analysis of non-covalent interactions

3.6.1. Reduced Density Gradient (RDG) analysis

The RDG analysis is a widely used tool to confirm the existence of non-covalent interactions and identify their types in molecular systems. The ED of the RDG as a function of (sign (λ_2)*ρ)) and iso-surface density gives us information about the nature and strength of the interactions that exist in the molecules which are classified into three types: H-bonding (strong NCI), vdW interactions (weak NCI) and steric effect (represent the repulsion between the atom of molecules) which are presented by a set of blue, green and red colors respectively [52]. The scatter graphs of 4PEKOX are shown in **Figure 7**. The function of (sign (λ_2)*ρ)) ranges between −0.05 and0.05 (a.u) in RDG scatter spectra, which are distributed as follows [53]:

- H-bonding interactions :(sign (λ_2)*ρ))< 0.
- vdWinteractions :(sign (λ_2)*ρ)) close to 0.
- Steric effects :(sign (λ_2)*ρ))>0.

As the RDG graph shows, the existence and distribution of NCI are well defined: H-bonding interactions (blue color) in the range [(−0.05)-(−0.015)]. The existence of vdW Interactions is confirmed by the green concentration in the graph between −0.015 and 0.01, the red color, on the other hand, represents atomic repulsion due to the steric effect that exists in the positive region between 0.01 and 0.05.

3.6.2. Atoms In Molecules (AIM) analysis

To make H-bonding interactions more visible through a visual approach, we performed the theory of AIM as presented in **Figure 8**.The objective is to identify the Critical Bonding Points (BCP) that result from the presence of these types of interactions [54]. The AIM is a useful approach for identifying types and strengths of H-bonds based on topological parameters that have been calculated and presented in **Table 5**.

The following categories can be used to classify H-bonding interactions [55]:

- Weak H-bonds: $\nabla^2\rho(r) > 0$ and $H(r) > 0$
- Moderate H-bonds: $\nabla^2\rho(r) > 0$ and $H(r) < 0$.
- Strong H-bonds: $\nabla^2\rho(r) < 0$ and $H(r) < 0$.

The Laplacian values of electron density $\nabla^2\rho(r)$and the Hameltonian kinetic energy H(r) show that the N-H...O H-bond ($\nabla^2\rho(r)>0$ and $H(r) < 0$) is stronger than the C-H...O bond ($\nabla^2\rho(r)>0$ and $H(r) > 0$) and therefore their contribution to the crystal packing and stabilization of this new compound is stronger, this can also be explained by the fact that the binding energy of N-H...O is higher than that of C-H...O **(Table 5)**.

3.7. Molecular Electrostatic Potential (MEP) surface

A visual tool for figuring out the relative polarity of compounds is the Molecular Electrostatic Potential (MEP) surface [56]. MEP surface is a 3D cartographic visualization of the charge distribution in a molecule. Negative sites are represented by red, positive sites by blue while green indicates the neutral region, so the signs of the sites represent the electrostatic potential

in terms of color grading [57]. **Figure 9** shows the MEP surface of 4PEKOX mapped using quantum chemical calculations, the red region is concentrated around the oxalate anion, while the blue region is concentrated on the organic cation, this well-defined color distribution is consistent with the relative donor-acceptor properties of the oxalate anion and 4-piperidinium ethyl ketal, respectively. This analytical result is a good indication of the reactivity that takes place between these two organic entities and the complexation between them through the establishment of non-covalent interactions, in particular hydrogen bonds, which are the most important factor for anion-cation attachment and therefore the stability of this new organic compound.

3.8. Mulliken Population Analysis

Mulliken population analysis is a method to describe the electronic distribution in molecules. This analysis allows us to determine the charge and electronegativity of each atom in the structure which provides a deep understanding of electronic transfer in the studied compounds [58]. The distribution of charges on the atoms shows the emergence of donor-acceptor pairs which cause the formation of non-covalent interactions, including the establishment of hydrogen bonds.

Table 6 shows the atomic charges for each atom of 4PEKOX, note that all carbon atoms of the organic cation other than C1 are negatively charged, as they are linked to two positively charged hydrogen atoms, C2 and C6 are the most electronegative, due to their attachment to the oxalate anion by C-H...O hydrogen bonds. The electronegativity of the N4 nitrogen atom is due to its protonation by a hydrogen atom from the oxalate anion. The oxalate anion's two carbon atoms are positively charged due to the fact that they are bonded to a pair of negatively charged oxygen atoms, O12 is the most electronegative oxygen atom in $(C_2O_4)^{2-}$, which can be explained by the proton transfer between it and N4 of 4-Piperidinium ethyl ketal and thus the creation of N-H...O type hydrogen bonds.

3.9. ELF, LOL and IRI analyses

To analyze non-covalent interaction from another point of view, we performed Electron Localized Function (ELF) and Local Orbital Locator (LOL) topological analyses, which were represented using Multiwfn software.The aim of these methods is to determine the location of electrons in the Lewis structure and show the existence of both bonding and non-bonding electrons [59]. The ELF map (**Figure 10a**) and LOL map (**Figure 10b**), displayed in the ranges of 0.0-0.1 and 0.0-0.8 respectively, show the concentration of the red color around the high electron localization, while the blue color surrounds the delocalized electron cloud. **Figure 10** shows that the concentration of red color around the indicated H-atoms of the organic cation and oxygen atoms of oxalate anion is relative to the intense electron localization around them, while the concentration of the blue color around the indicated carbon and nitrogen atoms of 4-Piperidinonium ethyl ketal shows the presence of a cloud of delocalized electrons, for the simple reason that these atoms are the H-bond donors. In the LOL map, the white area surrounding the hydrogen atom signifies that the electron density is above the scale limit [0.0-0.8].

The Interaction Region Indicator (IRI) study can be a complementary analysis to the ELF and LOL analyses, classifying Non-Covalent Interactions (NCLIs) that are established between anion-cationinto H-bonds, vdW and steric effect according to a group of colors that are blue, green and red respectively [60], as shown in **Figure 11**.

3.10. Molecular docking study

The application of supramolecular chemistry to the study of chemical biology therefore requires compounds synthesized by combining single molecules with the aim of complexing and linking them by non-covalent interactions. The discovery of drugs based on supramolecular chemistry shows high interactions with proteins, inhibiting their functions and mobilization [61,62].

Molecular docking is an effective approach for studying binding orientations and clarifying molecular mechanisms for ligands in the active regions of target proteins [59]. The 3D crystal structure of SARS-CoV-2 (7JTL) was obtained from the RCSB protein data bank, the structures of favipiravir, oxalic acid and 4-piperidinone ethyl ketal are obtained from the PubChem database, Single-crystal X-ray diffraction data of 4PEKOX were used for this analysis. Using iGEMDOCK program, the best-docked poses of 4PEKOX, favipiravir, oxalic acid and 4-piperidinone ethyl ketalwith the SARS-CoV-2 (7JTL) protein have been identified and illustrated in **Table 7**, then plotted in **Figure 12** and **Figure 13** using Discovery Studio to show the best docked positions, and the 3D interactions between ligands and protein.

As is evident, the complex 4PEKOX-SARS-CoV-2 has the highest binding affinity, as present in **Table 7** and shown in **Figure 13**, because it combines the strongest total energy (in absolute value) -81.5053 kcal.mol^{-1}, the strongest H-Bonds -18.5388 kcal.mol^{-1} and van der Waals interactions -63.8497 kcal.mol^{-1} in comparison to Oxalic acid-SARS-CoV-2 (Total energy = -48.4515 kcal.mol^{-1}; H-Bonding interactions = -14 kcal.mol^{-1}; VdW interactions = -35.4149 kcal.mol^{-1}) and 4-Piperidinone ethyl ketal-SARS-CoV-2 (Total energy=-59.607 kcal.mol^{-1}; H-Bonding interactions = -6.94099 kcal.mol^{-1}; VdW interactions = -52.666 kcal.mol^{-1}). The 3D representation shows the interactions between our compounds and SARS-CoV-2, which has five non-covalent bonds divided into three hydrogen bonds with the amino acidsA:LEU98 (one H-bond) and A:ARG115 (two H-bonds) combined with two electrostatic interaction(attractive charge interaction) with A:ARG115.

Favipiravir is an orally available antiviral agent active against SARS-CoV-2 [63,64]. We note that 4PEKOX-SARS-CoV-2 has a total energy higherthenFavipiravir-SARS-CoV-2 (Total energy = -71.3015 kcal.mol^{-1}), which presents the improvement of biological properties that requires the attachment by non-covalent interactions to produce supramolecules.

The deduction that can be drawn from this is the role of non-covalent interactions in the synthesis of supramolecules and their more interesting properties than the initial reagents. What has been confirmed by this analysis is the interaction behavior of this supramolecule with one of the most dangerous viruses, which became with a higher total energy than the reference (favipiravir) we chose, while the starting products (oxalic acid and 4-Piperidinone ethyl ketal) have lower energies than favipiravir.

4. Conclusion

The work presented in this manuscript has been oriented towards the synthesis of new purely organic crystal 4PEKOX. According to the crystallographic examination, this novel substance crystallizes in a monoclinic cell with the space group $P2_1/c$. The projection of the structure shows that the binding between 4-piperidinone ethyl ketal cations and oxalate anions is ensured by hydrogen bonds of type N-H...O and C-H...O which forms new supramolecular units: $R_2^2(8)$, $R_2^1(5)$ and $R_2^1(6)$. The spectroscopic analysis allowed us to determine the absorption band, electron transitions and vibrational properties related to the functional groups of 4PEKOX.

In another part, we performed quantum chemical calculations that allowed us to confirm the results obtained from the data collection through a theoretical analysis that studied in depth the non-covalent interactions responsible for the crystal formation of this new compound. The study of non-covalent interactions shows us the stability and the strong attachment between the two organic units which gave its fruit to produce this new organic compound.

The perspective of this work is the research that should be done in the synthesis of purely organic compounds in order to produce supramolecules with the aim of improving their properties and obtaining products with the desired characteristics, the good example being the interesting biological properties that you have acquired 4PEKOX in comparison with their starting reagents and in comparison with favipiravir, taking into account that favipiravor is a drug that is already being used against SARS-CoV-2, and that 4PEKOX has been developed to compete with it in terms of its energy of interaction against the virus. These results open up a wide range of researchthat should be directed towards the synthesis of this type of supramolecules to produce a material applicable in the targeted field, which combines the properties of the starting reagents and also with more interesting proprieties than it.

Acknowledgements

This work was supported by the Tunisian National Ministry of Higher Education and Scientific Research and Researchers Supporting Project number (RSP2023R61), King Saud University, Riyadh,Saudi Arabia. This study was partially carried out within the state assignment no. 0287-548 2021-0012 for the Institute of Chemistry and Chemical Technology, Siberian Branch of the Russian Academy of Sciences.

References

[1] O.A. Geras'ko, D.G. Samsonenko, V.P. Fedin, Supramolecular chemistry of cucurbiturils, Russ. Chem. Rev., 71 (2002) 471-460.

[2] A. Nangia, Supramolecular chemistry and crystal engineering, J. Chem. Sci., 122 (2010) 295-310.

[3] S. Kansız, N. Dege, Synthesis, crystallographic structure, DFT calculations and Hirshfeld surface analysis of a fumarate bridged Co(II) coordination polymer, J. Mol. Struct., 1173 (2018) 42-51.

[4] S. Kansız, A.M. Qadir, N. Dege, S.H. Faizi, Two new copper (II) carboxylate complexes based on N,N,N',N'-tetramethylethyleneamine: Synthesis, crystal structures, spectral properties, dft studies and hirshfeld surface analysis, J. Mol. Struct., 1230 (2021) 129916.

[5] Ö. Tamer, H. Mahmoody, K.F. Feyzioğlu, O. Kılınç, D. Avci, O. Orun, N. Dege, Y. Atalay, ynthesis of the first mixed ligand Mn (II) and Cd (II) complexes of 4-methoxy-pyridine-2-carboxylic acid, molecular docking studies and investigation of their anti-tumor effects in vitro, Appl. Organomet. Chem., 34 (2020) e5416.

[6] Q. Zhu, S. Hattori, Organic crystal structure prediction and its application to materials design, J. Mater. Res., 38 (2022) 19-36.

[7] J. Chen, B. Sarma, J.M.B. Evans, A.S. Myerson, Pharmaceutical Crystallization, Cryst. Growth Des., 11 (2011), 887–895.

[8] T. Li, A.Mattei, Pharmaceutical Crystals: Science and Engineering, (2008).

[9] B.A. Palmer, D. Gur, S. Weiner, L.Addadi, D.Oron, The Organic Crystalline Materials of Vision: Structure–Function Considerations from the Nanometer to the Millimeter Scale, Adv. Mater., 30 (2018) 1800006.

[10] J.S. Brooks, Organic crystals: properties, devices, functionalization and bridgesto bio-molecules, 39 (2010) 2667–2694.

[11] S.Panchapakesan, K. Subramani, B. Srinivasan, Growth, characterization and quantum chemical studies of an organic single crystal: 3-Aminopyridine 4-Nitrophenol for opto-electronic applications, J. Mater. Sci.: Mater. Electron., 28 (2017) 5754–5775.

[12] P. Yu, Y. Zhen, H. Dong, W. Hu, Crystal Engineering of Organic Optoelectronic Materials, Chem, 5 (2019) 2814-2853.

[13] Z. Cai, Z. Wang, J. Kim, Y. Yamauchi, Hollow Functional Materials Derived from Metal–Organic Frameworks: Synthetic Strategies, Conversion Mechanisms, and Electrochemical Applications, Adv Mater., 31 (2019) 1804903.

[14] A. Al-Mulla, A Review: Biological Importance of Heterocyclic Compounds,Der Pharma Chemica, 9 (2017) 141-147.

[15] M. S. Saini, A. Kumar, J.Dwivedi, R. Singh, A review: biological significances of heterocyclic compounds, Int. J. Pharm. Sci. Res., 4 (2013) 66-77.

[16] T. Yang, X. Cui, M. Tang, W. Qi, Z. Zhu, M. Shi, L. Yang, H. Pei, W. Zhang, L.xie, Y. Xu, Z. Yang, L. Chen, Identification of a Novel 2,8-Diazaspiro[4.5]decan-1-one Derivative as a Potent and Selective Dual TYK2/JAK1 Inhibitor for the Treatment of Inflammatory Bowel Disease, J. Med. Chem., 65 (2022) 3151–3172.

[17] A.Srinivas, A. Nagaraj, C.S. Reddy, Synthesis and nematicidal activity of 2-(1H-benzo[d]imidazol-2-ylmethyl)-4- aryl-1-thia-4-azaspiro[4.5]decan-3-one, Indian J. Chem., 47B (2008) 787-791.

[18] N.Onul, O.Ertik, N.Mermer, R.Yanardag, Synthesis and antioxidant, antixanthine oxidase, and antielastase activities of novel N,S-substituted polyhalogenated nitrobutadiene derivatives, J. Biochem. Mol. Toxicol., 32 (2018) e22021.

[19] J. Obniska, K. Kamiński, Synthesis and anticonvulsant properties of new N-phenylamino derivatives of 2-azaspiro[4.4]nonane, 2-azaspiro[4.5]decane-1,3-dione and 3-cyclohexylpyrrolidine-2,5-dione. Part IV, Acta Pol. Pharm., 63 (2006) 101-108.

[20] B.W. Strobel, Influence of vegetation on low-molecular-weight carboxylic acids in soil solution—a review, Geoderma, 99 (2001) 169-198.

[21] F. Palmieria, A. Estoppeya, G.L. Houseb,A.Lohbergera, S.Bindschedlera, P.S.G. Chainb,P.Junier, Oxalic acid, a molecule at thecrossroads of bacterial-fungal interactions, Adv. Appl. Microbiol., Adv. Appl. Microbiol., 106 (2019) 49-77.

[22] K. Mahendra, N.K. Udayashankar, Growth and comparative studies on oxalic acid dihydrate, potassium oxalate hydrate and potassium hydrogen oxalate oxalic acid dihydrate single crystals, J. Phys. Chem. Solids., 138 (2020) 109263.

[23] M. Çalişkan, The Metabolism of Oxalic Acid, Turk. J. Zool., 24 (2000) 103-106.

[24] D.S. Robertson, The function of oxalic acid in the human metabolism, The function of oxalic acid in the human metabolism, Clin. Chem. Lab. Med., 49 (2011) 1405–1412.

[25] S. Noonan, G. Savage, Oxalate content of foods and its effect on humans, Asia Pac J ClinNutr., 8 (1999) 64-67.

[26] L. J. Farrugia, WinGX and ORTEP for Windows: an update, J. Appl. Cryst., 45 (2012) 849-854.

[27] G.M. Sheldrick, Crystal structure refinement with SHELXL. ActaCrystallogr., 71 (2015) 3–8.

[28] R. Dennington, T. Keith, J. Millam, GaussView, Version 5, Semichem. Inc, Shawnee Mission, KS, USA, 2009.

[29] M.J. Frisch, G.W. Trucks, H.B. Schlegel, G.E Scuseria, M.A Robb, J.R Cheeseman, G. Scalmani, V. Barone, B. Mennucci, G.A. Petersson and al. Gaussian 09, Revision C.01, Gaussian, Inc.: Wallingford, UK, 2009.

[30] J. Tirado-Rives, W.L. Jorgensen, Performance of B3LYP Density Functional Methods for a Large Set of Organic Molecules, J. Chem. Theory Comput., 4 (2008) 297-306.

[31] S.Scheiner, Comparison of Various Means of Evaluating Molecular Electrostatic Potentials for Noncovalent Interactions, J. Comput. Chem., 39 (2017) 500-510.

[32] I.Sidir, Y. G. Sidir, M. Kumalar, E. Tasal, Ab initio Hartree–Fock and density functional theory investigations on the conformational stability, molecular structure and vibrational spectra of 7-acetoxy-6-(2,3-dibromopropyl)-4,8-dimethylcoumarin molecule, J. Mol. Struct., 964 (2010) 134-151.

[33] Ramalingam, A., Sambandam, S., Medimagh, M., Al-Dossary, O., Issaoui, N., & Wojcik, M. J. (2021). Study of a new piperidone as an anti-Alzheimer agent: Molecular docking, electronic and intermolecular interaction investigations by DFT method. Journal of King Saud University-Science, 33(8), 101632.

[34] M. Jemai, S. Gatfaoui, N. Issaoui, T. Roisnel, A. S.Kazachenko, O. Al-Dossary, H. Marouani, A.S. Kazachenko, Synthesis, Empirical and Theoretical Investigations on NewHistaminiumBis(Trioxonitrate) Compound, Molecules, 28 (2023) 1931.

[35] S.D. Kanmazalp, M. Macit, N. Dege, Hirshfeld surface, crystal structure and spectroscopic characterization of (E)-4-(diethylamino)-2-((4-phenoxyphenylimino)methyl)phenol with DFT studies, J. Mol. Struct., 1179 (2019) 181-191.

[36] W. Guerrab , Ill-Min Chung, S. Kansiz, J.T. Mague, N. Dege, J. Taoufik, R. Salghi, I.H. Ali , M.I. Khan, H. Lgaz , Y. Ramli, J. Mol. Struct., 1197 (2019) 369-376.

[37] M. Evecen, H. Tanak, F. Tinmaz, N. Dege, İ.Ö. İlhan, Experimental (XRD, IR and NMR) and theoretical investigations on 1-(2-nitrobenzoyl)3,5-bis(4-methoxyphenyl)-4,5-dihydro-1H-pyrazole, J. Mol. Struct., 1126 (2016) 117-126.

[38] I.M. Khan, M. Islam, S. Shakya, N. Alam, S. Imtiaz, M.R. Islam, Synthesis, spectroscopic characterization, antimicrobial activity, molecular docking and DFT studies of proton transfer (H-bonded) complex of 8-aminoquinoline (donor) with chloranilic acid (acceptor), J. Biomol. Struct. Dyn., 40 (2021), 12194-12208.

[39] S. Shakya, I.M. Khan, B. Shakya, Y.H. Siddique, H. Varshney, S. Jyotib, Protective effect of the newly synthesized and characterized charge transfer (CT) complex against arecoline induced toxicity in third-instar larvae of transgenic Drosophila melanogaster (hsp70-lacZ)Bg9: experimental and theoretical mechanistic insights, J. Mater. Chem. B, 11 (2023) 1262-1278.

[40] I.M. Khan, A. Naeem, A. Ahmad, Semiquantitative determination of some nitrogen compounds by the formation of charge-transfer complexes of diphenylamine with p-dimethylaminobenzaldehyde by capillary solid-state spot-tests, Chin. Chem. Lett., 21 (2020) 720-724.

[41] I.M. Khan, A. Khan, S. Shakya, M. Islam, Exploring the photocatalytic activity of synthesized hydrogen bonded charge transfer co-crystal of chloranilic acid with 2-ethylimidazole: DFT, molecular docking and spectrophotometric studies in different solvents, J. Mol. Struct., 1277 (2023) 134862.

[42] J. Bernstein, Polymorphism of L-glutamic acid: decoding the [alpha]-[beta] phase relationship via graph-set analysis, ActaCryst., B74 (1991) 1004-1010.

[43] M. A. Spackman, D. Jayatilaka, Hirshfeld surface analysis, CrystEngComm. 11 (2009) 19-32.

[44] M. A. Spackman, J. J. Mckinnon, Fingerprinting intermolecular interactions in molecular crystals, CrystEngComm, 4 (2002) 378-392.

[45] M.Jemai, M. Khalfi, N. Issaoui, T. Roisnel, A.S. Kazachenk, O. Al-Dossary, H. Marouani, A. S. Kazachenko, Y. N. Malyar, Role of Non-Covalent Interactions in Novel SupramolecularCompound, Bis(4-phenylpiperazin-1-ium) Oxalate Dihydrate:Synthesis, Molecular Structure, Thermal Characterization,Spectroscopic Properties and Quantum Chemical Study, Crystals, 13 (2023) 875.

[46] H.Dhaouadi, H. Marouani, M. Rzaigui, S. S. Al-Deyab, A. Madani, Crystal Structure and Spectroscopic Investigations of a New Organic Monophosphate Monohydrate, Phosphorus Sulfur Silicon Relat. Elem., 185 (2010) 609-619.

[47] H. Marouani, M. Rzaigui, S. S. Al-Deyab, Synthesis and Characterization of Tetrakis(4-oxo-piperidinium ethylene acetal) Bis Sulfate Hexahydrate,J. Chem.,8 (2011) 1930-1936.

[48] K. I. Peterson, D. P. Pullman, Determining the Structure of Oxalate Anion Using Infrared andRaman Spectroscopy Coupled with Gaussian Calculations, J. Chem. Educ., 93 (2016) 1130−1133.

[49] J. Tauc, Optical properties and electronic structure of amorphous Ge and Si, Mater. Res. Bull., 3 (1968) 37-46.

[50] M. Medimagh, N. Issaoui, S. Gatfaoui, O. Al-Dossary, A.S. Kazachenko, H. Marouani, M.J. Wojcik, Molecular modeling and biological activity analysis of new organic-inorganic hybrid: 2-(3,4-dihydroxyphenyl) ethanaminium nitrate, J. King Saud Univ. Sci., 33 (2021) 101616.

[51] S. Gatfaoui, N. Issaoui, S.A. Brandán, M. Medimagh, O. Al-Dossary, T. Roisnel, H. Marouani, A. S. Kazachenko, Deciphering non-covalent interactions of 1,3-Benzenedimethanaminiumbis(trioxonitrate): Synthesis, empirical and computational study, J. Mol. Struct., 1250 (2022) 131720.

[52] S. Gatfaoui, N. Issaoui, A. S. Kazachenk, O. Al-Dossary, T. Roisnel, H. Marouani, Synthesis, characterization and identification of inhibitory activity on the main protease of COVID-19 by molecular docking strategy of (4-oxo-piperidinium ethylene acetal) trioxonitrate, J. King Saud Univ. Sci., 35 (2023) 102758.

[53] S. Gatfaoui, N. Issaoui, T. Roisnel, H. Marouani, A proton transfer compound template phenylethylamine: Synthesis, a collective experimental and theoretical investigations, J. Mol. Struct., 1191 (2019) 183-196.

[54] S. Gatfaoui, N. Issaoui, T. Roisnel, H. Marouani, Synthesis, experimental and computational study of a non-centrosymmetric material 3-methylbenzylammonium trioxonitrate, J. Mol. Struct., 1225 (2021) 129132.

[55] F. Akman, N. Issaoui, A. Kazachenko, Intermolecular hydrogen bond interactions in the thiourea/water complexes (Thio-(H_2O)n) (n=1, . . . , 5): X-ray, DFT, NBO, AIM, and RDG analyses, .J. Mol. Model., 26 (2020) 161.

[56] E. Scrocco, J. Tomasi, Reactivity and Intermolecular Forces: An Euristic Interpretationby Means of Electrostatic Molecular Potentials, Adv. Quant. Chem. 11 (1978) 115-193

[57] P. Thul, V.P. Gupta, V.J. Ram, P. Tandon, Structural and spectroscopic studies on 2-pyranones,Spectrochim. Acta 75 (2010) 251-260.

[58] Z. Qu, F. Sun, X. Pi, H. Wang, X. Li, J. Gao, G. Zhao, Revealing the activity origin of oxygen-doped amorphous carbon material for SO2 catalytic oxidation: A descriptor considering dynamic electron transfer during O2 activation, Carbon, 201 (2023) 37-48.

[59] M. Medimagh, C. Ben Mleh, N. Issaoui, A.S. Kazachenko,T.Roisnel, O. M. Al-Dossary, H. Marouani, L.G. Bousiakoug, DFT and molecular docking study of the effect of a green solvent (waterand DMSO) on the structure, MEP, and FMOs of the 1-ethylpiperazine-1,4-diium bis(hydrogenoxalate) compound, J. Mol. Liq., 369 (2023) 120851.

[60] M. Medimagh, N. Issaoui, S. Gatfaoui, A.S. Kazachenko,O. M. Al-Dossary, N. Kumar,H. Marouani, L.G. Bousiakoug, Investigations on the non-covalent interactions, drug-likeness,molecular docking and chemical properties of 1,1,4,7,7-pentamethyldiethylenetriammoniumtrinitrate by density-functionaltheory, J. King Saud Univ. Sci., 35 (2023) 102645.

[61] D.A. Uhlenheuer, K. Petkaua, L. Brunsveld,Combining supramolecular chemistry with biology, Chem. Soc. Rev., 39 (2010) 2817-2826.

[62] S. Sakamoto, K. Kudo, Supramolecular Control of Split-GFP Reassembly by Conjugation of β-Cyclodextrin and Coumarin Units, J. Am. Chem. Soc., 130 (2008) 9574-9582.

[63] J. Santos, S. Brierley, M.J. Gandhi, M.A. Cohen,P.C.Moschella, A.B. L. Declan, Repurposing Therapeutics for Potential Treatmentof SARS-CoV-2: A Review, Viruses, 12 (2020) 705.

[64] M. Sada, T. Saraya, H. Ishii, K. Okayama, Y. Hayashi,T.Tsugawa, A. Nishina, K. Murakami, M. Kuroda, A. Ryo, H. Kimura, Detailed Molecular Interactions of Favipiravir withSARS-CoV-2, SARS-CoV, MERS-CoV, and InfluenzaVirus Polymerases InSilico, Microorganisms, 8 (2020) 1610.

Figure captions

Fig. 1. Ortep representation with atom-labeling scheme, displacement ellipsoids are drawn at the 50% probability level **(a)** and optimized structure **(b)** of **4PEKOX**. Symmetry code (i): -x, -y, -z

Fig.2. Projection of the **4PEKOX** structure along the ($\vec{a}$, $\vec{c}$) plane**(a)** and the attachment of oxalate anions and 4-Piperidinonium ethyl ketal cations by hydrogen bonds N-H...O and C-H...O**(b)**.

Fig.3. Hirshfeld surface mapped overd_{norm} mode and its two-dimensional fingerprint plotsof the title compound **(a)**, and its cation **(b)** and anion **(c)**.

Fig. 4. Infrared absorption spectrum of **4PEKOX**.

Fig. 5. Ultraviolet absorption spectrum of **4PEKOX (a)** and determination of the gap energy obtained via the Tauc model **(b)**.

Fig.6. Molecular frontier orbitals of **4PEKOX**.

Fig.7. Reduced density gradient scatter(a) and iso-surface density of**4PEKOX** to show the non-covalent interactions.

Fig.8. Graphical display of AIM analysis of **4PEKOX** (the critical binding points (BCP) and the connection paths are represented respectively by small balls and orange lines).

Fig.9. Molecular Electrostatic Potential Surface (MEPS) of **4PEKOX**.

Fig.10. Plotting maps for the **4PEKOX**'s ELF and LOL.

Fig.11. Plotting maps for the **4PEKOX**'s IRI.

Fig.12. Best poses of protein-ligand interaction.

Fig.13. 3D interactions of **4PEKOX**, favipiravir, oxalic acid and 4-Piperidinone ethyl ketal with the SARS-CoV-2 (7JTL) protein.

Fig.1

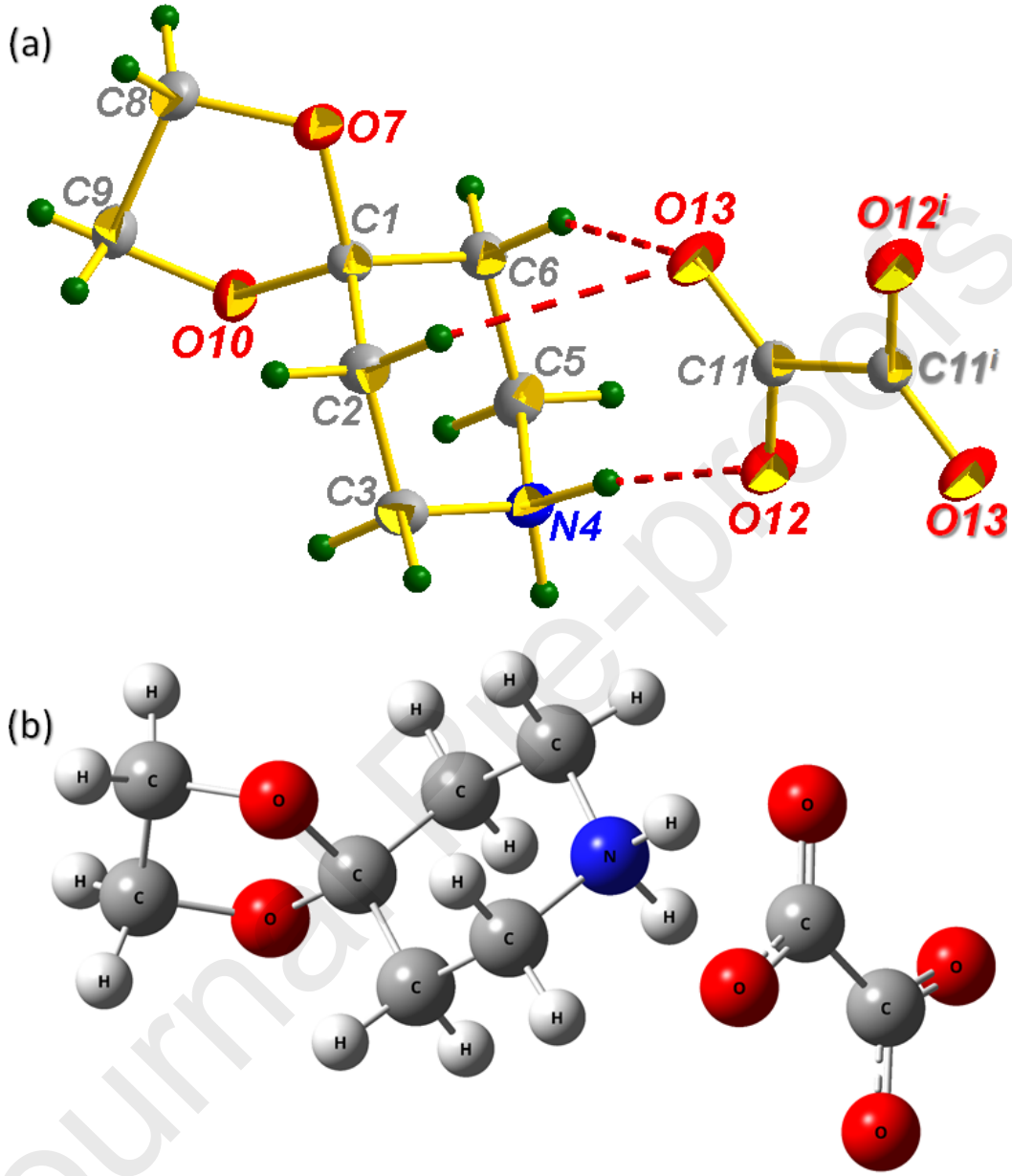

Fig.2

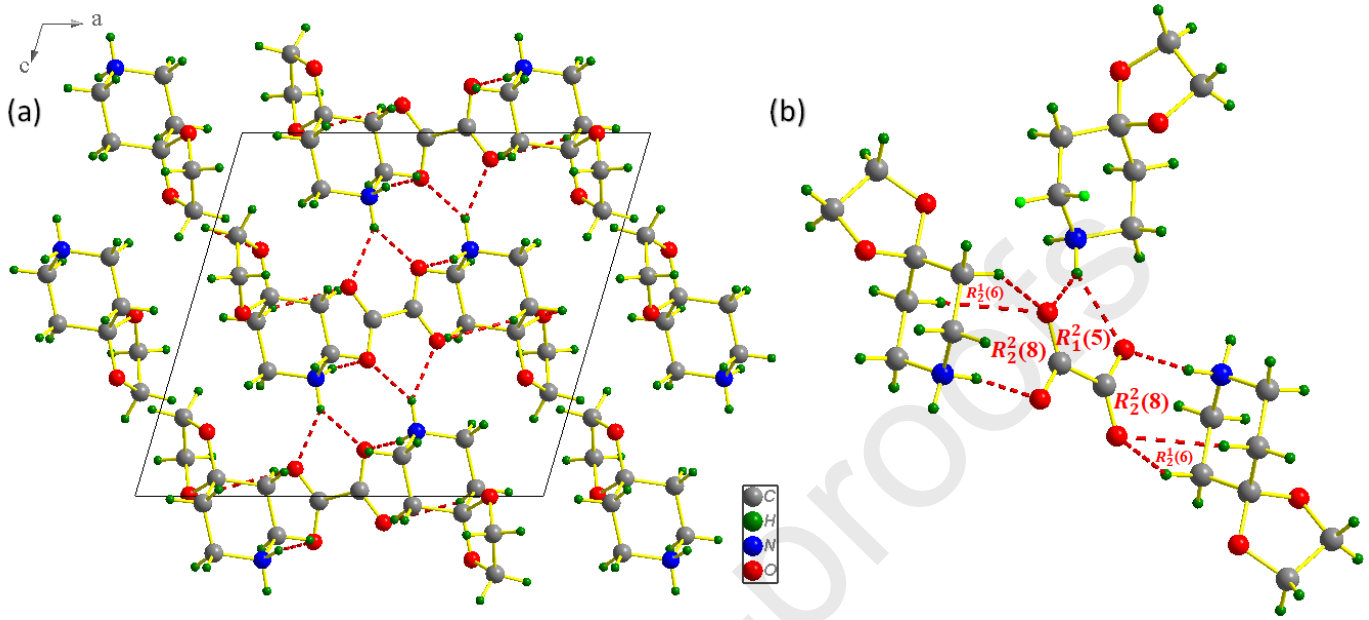

Fig.3

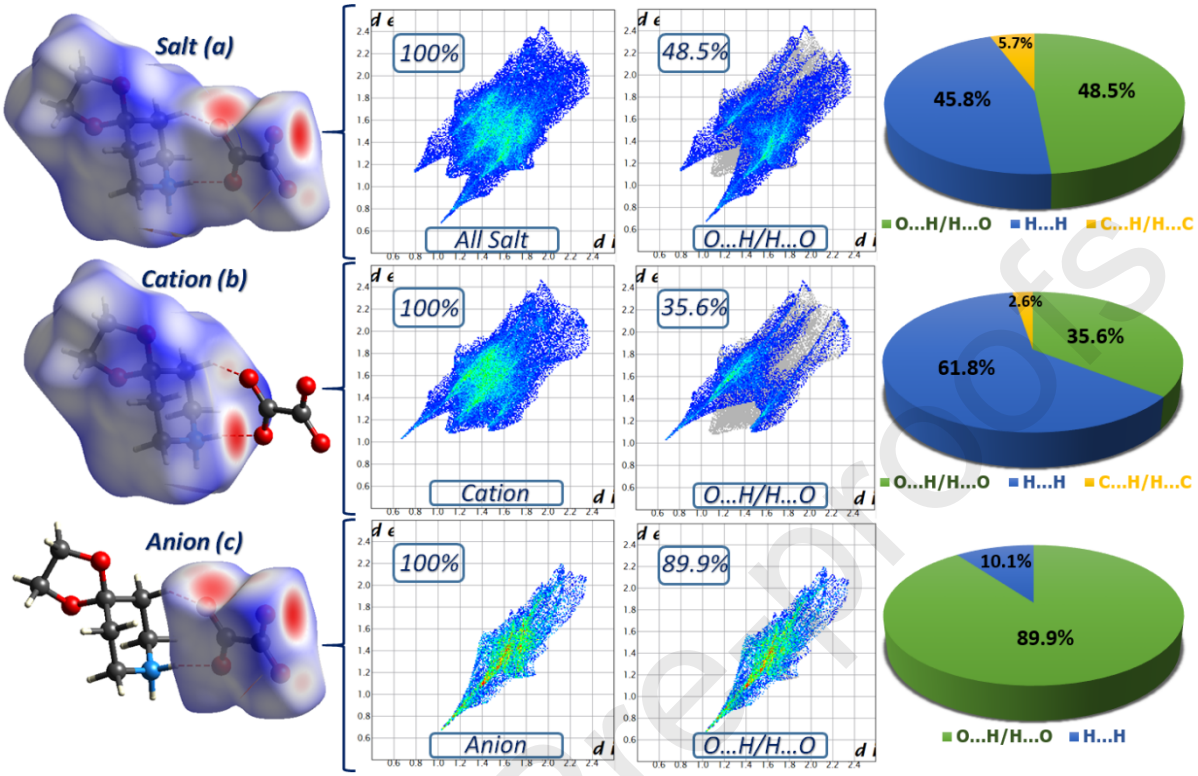

Fig. 4.

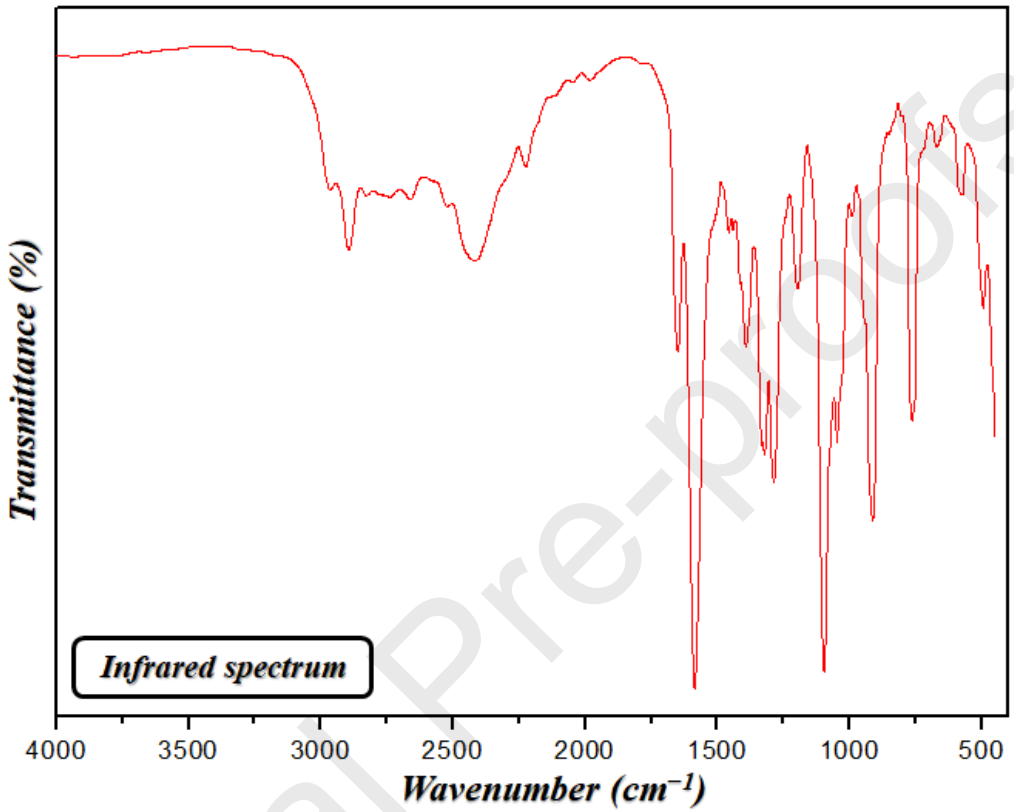

Fig.5

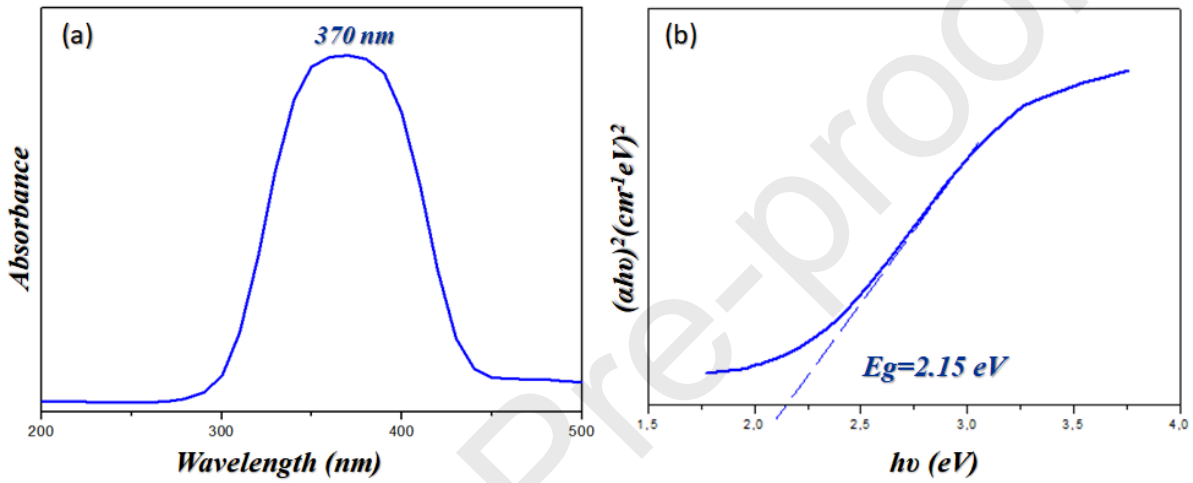

Fig.6

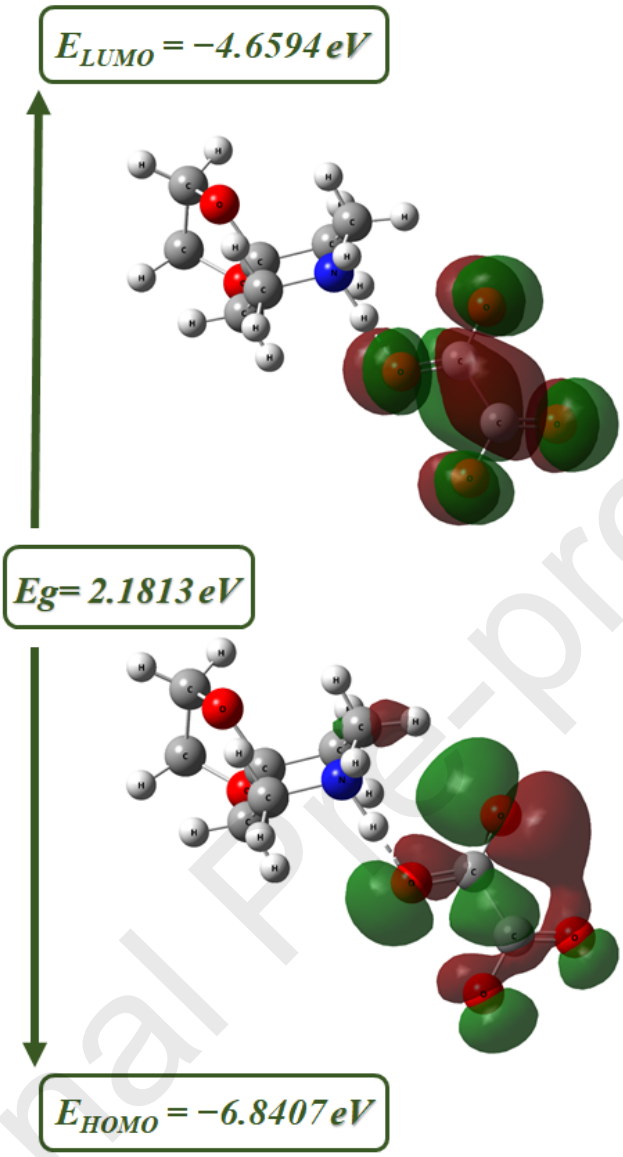

Fig.7

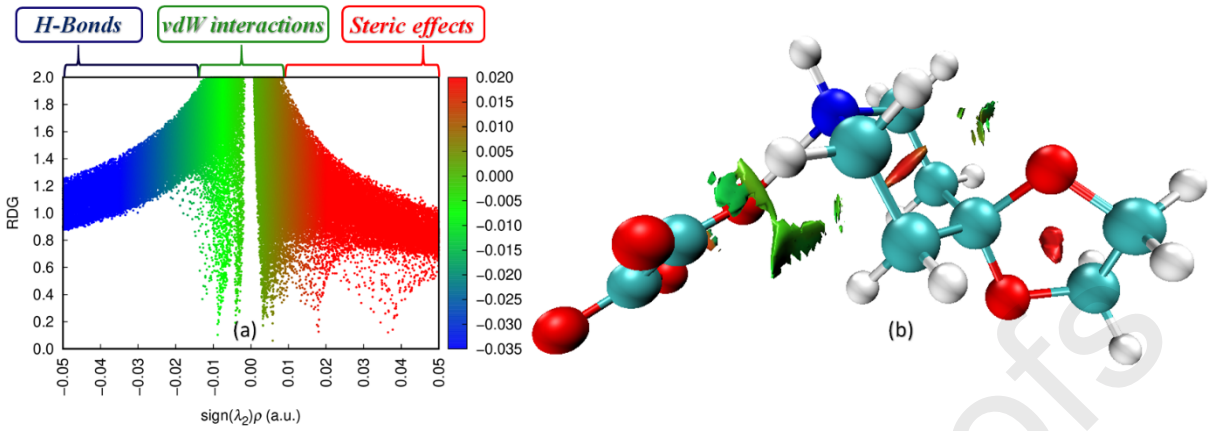

Fig.8

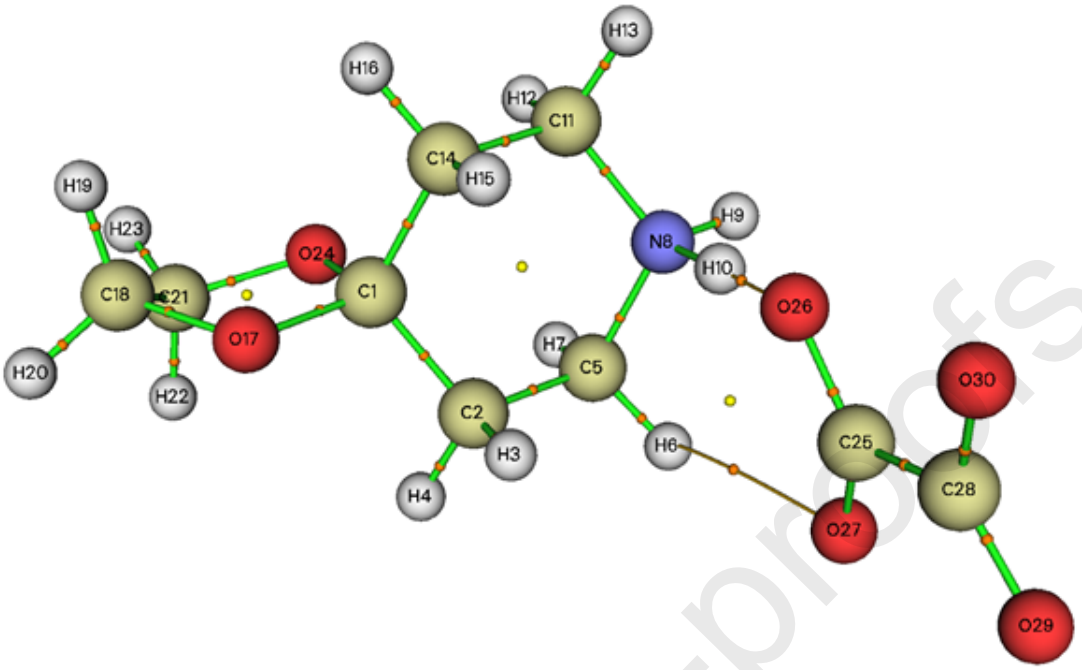

Fig.9

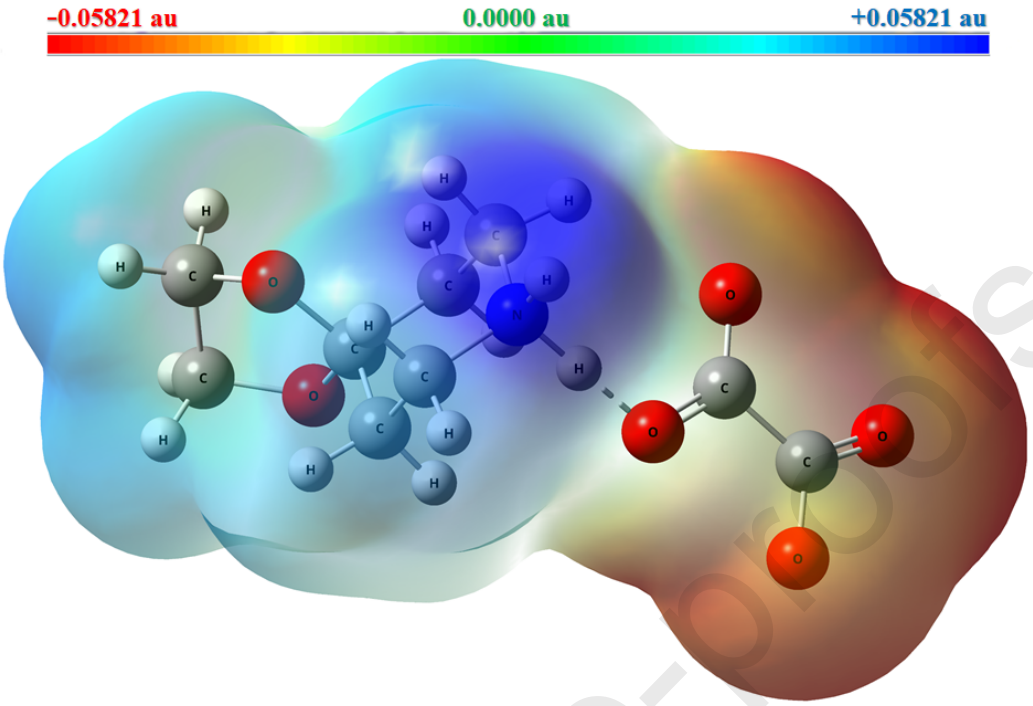

Fig. 10

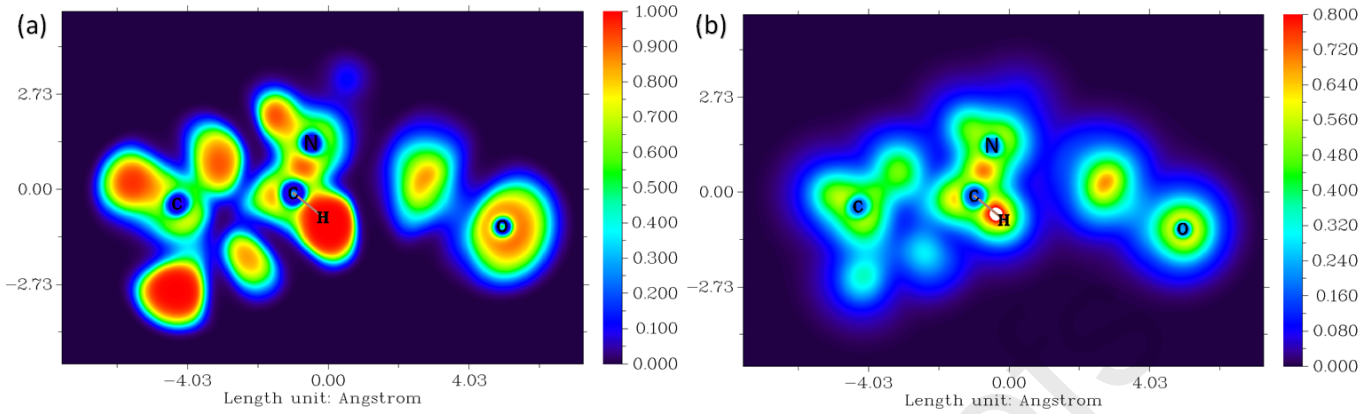

Fig. 11

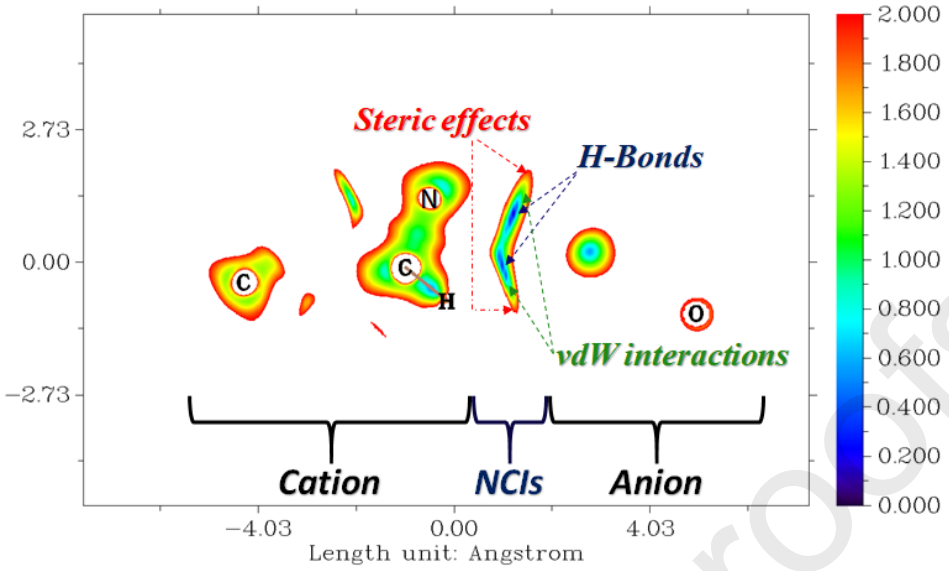

Fig.12

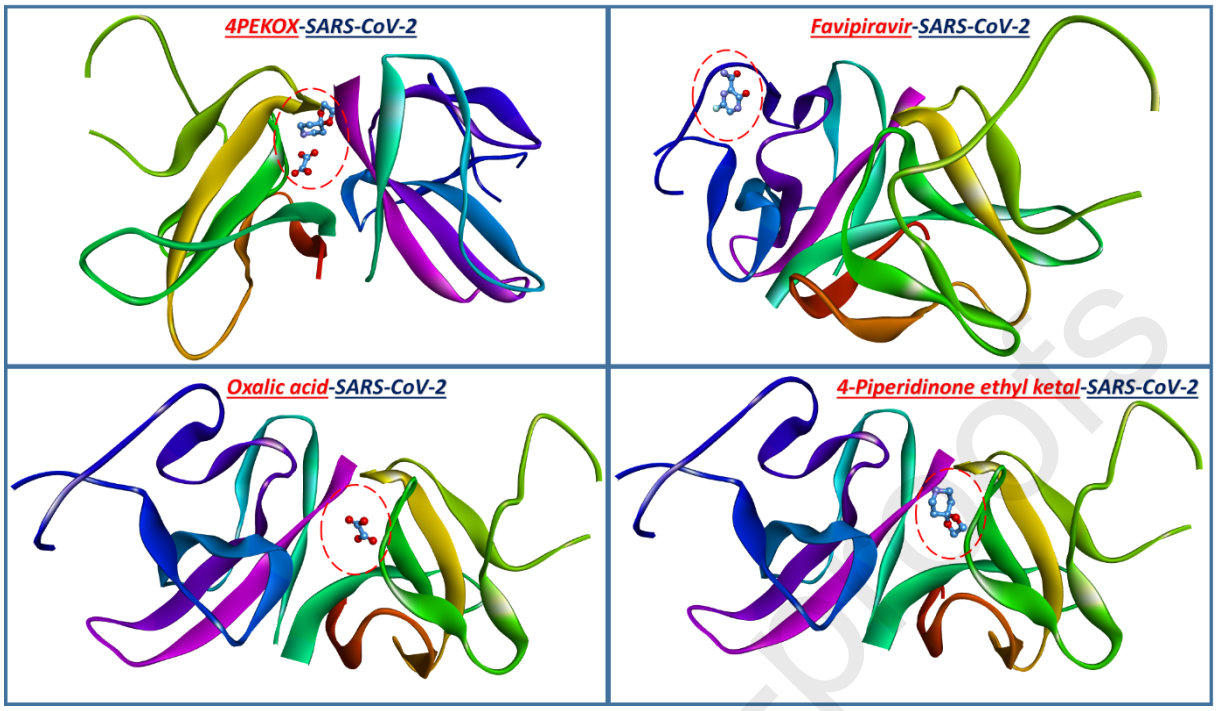

Fig.13

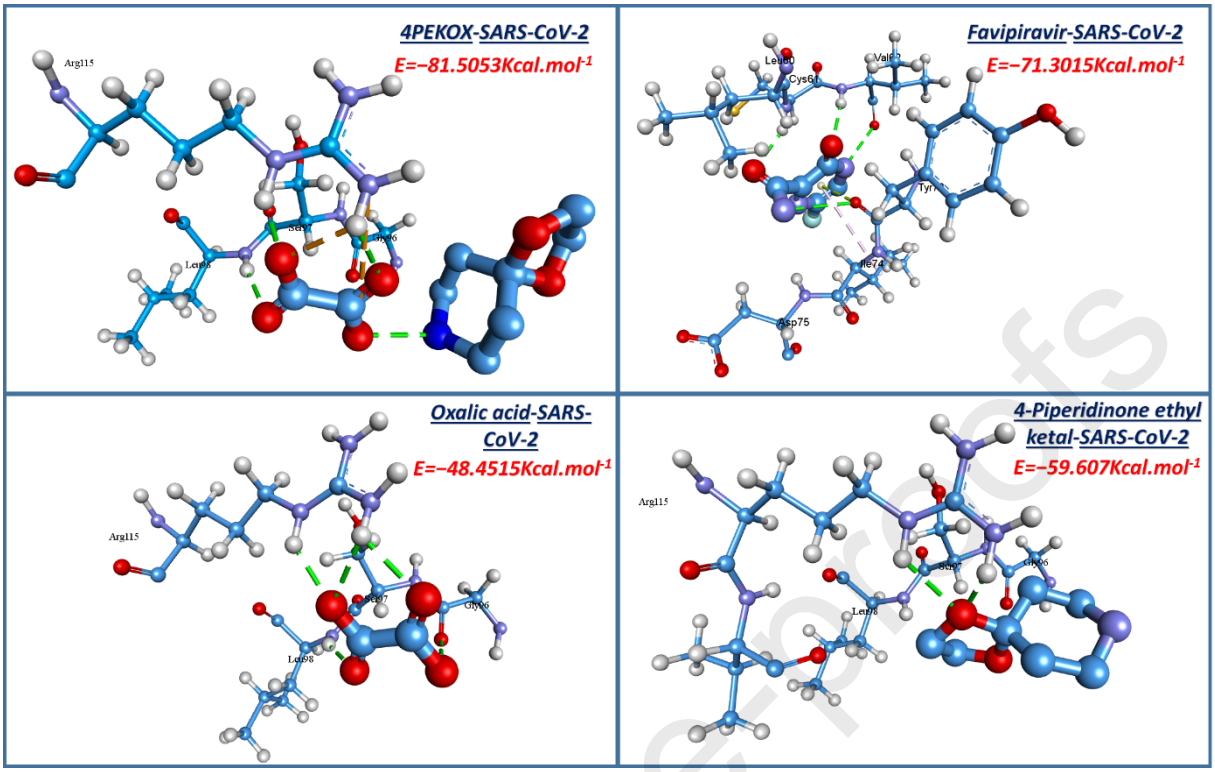

Table 1. Crystal data of the new bis(4-Piperidinonium ethyl ketal) oxalate

CCDC Number	**2269990**
Temperature	150 K
Empirical formula	$(C_7H_{14}NO_2)_2(C_2O_4)$
Formula weight (g mol^{-1})	376,40
Crystal size (mm)	0.27 × 0.12 × 0.05
Crystal system	monoclinic
Space group	$P2_1/c$
a(Å)	12.1401 (8)
b(Å)	6.9253 (5)

c(Å)	11.2564 (7)
β(°)	106.433 (2)
Z	2
V(Å^3)	907.71 (11)
F (000)	404
Mo Kα (mm^{-1})	μ= 0.11
Reflections collected	6766
Independent reflections	2072
Reflections with I > 2σ(I)	1913
R_{int}	0.028
Absorption correction:	*multi-scan* T_{min}= 0.954 ,T_{max}= 0.995
Refined parameters	124
R[F^2 > 2s(F^2)]	0.033
wR(F^2)	0.089
Goodness-of-fit on F^2	1.057

Table 2. Principal distances (Å) and bond angles (°) in 4PEKOX

Parameters	[r]	**Calculated**
	Bond length (Å)	
$(C_7H_{14}NO_2)^+$		
C1—O7	1.4250 (12)	1.4816
C1—O10	1.4259 (12)	1.4625
C1—C6	1.5154 (14)	1.5328
C1—C2	1.5231 (14)	1.5351
C2—C3	1.5198 (14)	1.5384
C3—N4	1.4901 (14)	1.5139
N4—C5	1.4861 (13)	1.5197
C5—C6	1.5186 (14)	1.5378
O7—C8	1.4289 (13)	1.4745
C8—C9	1.5191 (15)	1.5382
C9—O10	1.4301 (12)	1.4731
$(C_2O_4)^{2-}$		
C11—O13	1.2435 (13)	1.2612
C11—O12	1.2582 (12)	1.313
C11—C11^{i}	1.5604 (19)	1.5356

Bond angle (°)		
$(C_7H_{14}NO_2)^+$		
O7—C1—O10	106.05 (8)	106.0473
O7—C1—C6	110.37 (8)	110.6922
O10—C1—C6	108.48 (8)	108.9433
O7—C1—C2	110.06 (8)	107.9967
O10—C1—C2	111.28 (8)	111.5931
C6—C1—C2	110.50 (8)	111.4382
C3—C2—C1	110.61(8)	110.3639
N4—C3—C2	111.05 (8)	109.6982
C5—N4—C3	113.17 (8)	113.5095
N4—C5—C6	111.14 (8)	110.2017
C1—C6—C5	110.85 (8)	111.1788
C1—O7—C8	108.62 (8)	107.9006
O7—C8—C9	104.35 (8)	102.7781
O10—C9—C8	102.49 (8)	102.7084
C1—O10—C9	105.43 (7)	108.2063
$(C_2O_4)^{2-}$		
O13—C11—O12	126.43 (9)	126.7961

O13—C11—C11^{i}	117.52 (11)	119.6947
O12—C11—C11^{i}	116.04 (11)	113.5092

Symmetry code: (i) −x+1, −y, −z+1.

Table 3. Geometry of hydrogen bonds (Å, °) in4PEKOX

D—H…A	**D—H (Å)**	**H…A (Å)**	**D…A (Å)**	**D—H…A (°)**
N4—H4A···O12^{ii}	0.941 (14)	2.140 (14)	2.8928 (12)	133.62 (11)
N4—H4A···O13^{iii}	0.941 (14)	1.975 (14)	2.7785 (12)	142.1 (11)
N4—H4B···O12	0.920 (14)	1.793 (14)	2.7045 (12)	170.2 (12)
C2—H2A···O13	0.99	2.56	3.4104 (13)	144
C6—H6A···O13	0.99	2.53	3.3873 (13)	145

Symmetry codes: (ii) –x+1, y+1/2, −z+3/2; (iii) x, −y+1/2, z+1/2

Table 4. Global reactivity energy parameters of 4PEKOX

E_{HOMO} (eV)	−6.8407
E_{LUMO} (eV)	−4.6594
$\lvert E_{HOMO} - E_{LUMO} \rvert$ Gap (eV)	2.1813
Ionization potential: $I = -E_{HOMO}$	6.8407
Electronic affinity: $A = -E_{LUMO}$	4.6594
Electronegativity : $\chi = (I + A)/2$	5.7
Chemical potential: $\mu = -(I + A)/2$	−5.7
Hardness : $\eta = (I - A)/2$	1.0906
Softness : $S = 1/2\eta$	0.4585
Global electrophilicity: $\omega = \mu^2/2\eta$	14.8955

Table 5. Topological parameters of 4PEKOX

Interactions	Density of all electrons ρ(r)	Laplacian of electron density ∇^2 ρ(r)	Potential energy density V(r)	Lagrangian kinetic energy G(r)	Hameltonian kinetic energy H(r)	Interaction energy (E_{int}) kJ.mol^{-1}
N8–H10...O26	0.1050	0.1295	-0.1220	0.0772	-0.0448	-160.14
C5–H6...O27	0.0089	0.0342	-0.0049	0.0067	0.0018	-6.41

Table 6. Atomic charges in 4PEKOX

$(C_7H_{14}NO_2)^+$	Atomic charge	$(C_2O_4)^{2-}$	Atomic charge
C1	0.393963	C11	0.112523
C6	-0.499571	O12	-0.428572
H6A	0.336470	O13	-0.298408
H6B	0.242173	$C11^i$	0.145813
C5	-0.437889	$O12^i$	-0.240327
H5A	0.281267	$O13^i$	-0.165546
H5B	0.281255		
N4	-0.388441		
H4A	0.363066		
H4B	0.443623		
C3	-0.451803		
H3A	0.287061		
H3B	0.283691		
C2	-0.493799		
H2A	0.325065		
H2B	0.260752		
O10	-0.307276		

C9	-0.320301	
H9A	0.241425	
H9B	0.243366	
C8	-0.363604	
H8A	0.228447	
H8B	0.265707	
O7	-0.340129	

Symmetry code: (i) −x+1, −y, −z+1.

Table 7. Molecular docking calculations of binding energies with SARS-CoV-2 (7JTL) protein (kcal.mol^{-1})

Ligand	Total energy	VDW	H-Bond	Elec
4PEKOX	-81.5053	-63.8497	-18.5388	0.883236
Oxalicacid	-48.4515	-35.4149	-14	0.963468
4-Piperidinone ethylketal	-59.607	-52.666	-6.94099	0
Favipiravir	-71.3015	-47.9817	-23.3198	0

Declaration of Interests

On behalf of our the authors I hereby declare that：

- ✓ there are no known conflicts of interest associated with this publication and there has been no significant financial support for this work that could have influenced its outcome.
- ✓ the manuscript has been read and approved by all named authors.

Prof. Dr. Noureddine ISSAOUI